Journal of Organometallic Chemistry 694 (2009) 2315–2318

Contents lists available at ScienceDirect

Journal of Organometallic Chemistry

journal homepage: www.elsevier.com/locate/jorganchem

Metallic osmium and ruthenium nanoparticles for CO oxidation

Chunxiang Li [a], Weng Kee Leong [a,*], Ziyi Zhong [b]

[a] Department of Chemistry, National University of Singapore, 3 Science Drive 3, Singapore 117543, Singapore
[b] Institute of Chemical and Engineering Sciences, 1 Pesek Road, Jurong Island, Singapore 627833, Singapore

ARTICLE INFO

Article history:
Received 2 March 2009
Received in revised form 23 March 2009
Accepted 23 March 2009
Available online 29 March 2009

Keywords:
Osmium
Ruthenium
Metallic nanoparticles
Cluster
CO oxidation

ABSTRACT

Supported metallic catalysts were prepared from pyrolysis of the organometallic clusters $RuOs_3(CO)_{13}(\mu\text{-}H)_2$, $Os_3(CO)_{10}(\mu\text{-}AuPPh_3)_2$, $Os_3(CO)_{12}$, $Ru_3(CO)_{12}$ and $[Ru(CO)_4]_n$, on either silica or titania, and their catalytic performance for CO oxidation has been assessed against a supported catalyst prepared from $RuCl_3$. Ruthenium catalysts prepared from organometallic precursors were found to exhibit better activity, and that supported on TiO_2 exhibited activity at the lowest operating temperature.

1. Introduction

CO oxidation, a relatively simple, irreversible reaction without parallel or secondary reactions, is probably the best studied heterogeneously catalysed reaction. That it is of relevance to problems such as the removal of CO from automotive exhaust and in industrial pollution abatement [1], has made the development of catalysts for fast and complete oxidation of CO at low temperatures an active area of research for the past several decades. The reaction is exothermic, but has a relatively high kinetic barrier [2].

$$CO + 1/2O_2 \rightarrow CO_2 \quad \Delta H^{\circ}_{298.15\,K} = -283\ \text{kJ mol}^{-1}$$

Among the most active catalysts for CO oxidation are the supported Au catalysts of Haruta [3]. Extremely fine, deposited gold particles have been reported to be very active at low temperatures. However, the activity depends critically on the particle size and is hence susceptible to sintering [4]. Other materials investigated include Ru [5], RuO_2 [6], CuO/CeO_2 [7], Pd [8], Pt [9,10], and alloys such as $Al_1Mn_{6.7}Co$, and $Ag_{3.3}Mn_{34.1}Co_{1.7}Ni$ [11]. Recent research has shown that hydrous ruthenium oxide is a very active catalyst for the oxidation of CO. However, this material suffers from decomposition upon heating [12]. The sol–gel method adopted afforded a material with high surface area, but the poor thermal stability and crystallinity limited its use [13].

A number of studies have shown that the use of organometallic clusters as precursors afforded metallic nanoparticles that are small, with a narrow size distribution, leading to significant improvement in catalytic efficiencies. They also afford good control in the case of bimetallic particle composition as in the precursors, the two metallic elements are mixed homogeneously at the atomic scale [14–16]. In this study, we have prepared a number of metal catalysts containing ruthenium, osmium and/or gold, from readily available organometallic precursors, and studied their catalytic efficiency with respect to CO oxidation.

2. Experimental

The compounds $RuOs_3(CO)_{13}(\mu\text{-}H)_2$ [17], $Os_3(CO)_{10}(\mu\text{-}H)(\mu\text{-}AuPPh_3)$ [18] and $[Ru(CO)_4]_n$ [19,20] were prepared according to the reported procedures. $Os_3(CO)_{12}$, $Ru_3(CO)_{12}$ and $RuCl_3$ were purchased from Oxkem and used as supplied without further purification.

2.1. General procedure for pyrolysis of organometallic clusters

The clusters were added to SiO_2 (Aerosil Degussa 200) or TiO_2 (Degussa P25) at roughly 7% loading by weight, flame-sealed in a tube after evacuation, and then heated for 24 h at 200 °C and for another 24 h at 400 °C. The individual mixtures were then reduced under a stream of hydrogen gas for 2 h at 400 °C and then cooled to room temperature. Prior to thermolysis, both supports were calcined overnight at 100 °C.

* Corresponding author. Current address: Division of Chemistry and Biological Chemistry, Nanyang Technological University, SPMS-04-01, 21 Nanyang Link, SPMS-CBC-06-07, Singapore 637371, Singapore.
E-mail address: chmlwk@ntu.edu.sg (W.K. Leong).

0022-328X/$ - see front matter © 2009 Elsevier B.V. All rights reserved.
doi:10.1016/j.jorganchem.2009.03.038

2.2. Preparation of $RuCl_3/SiO_2$ catalyst

Silica powder (700 mg) was added to an ethylene glycol (100 ml) solution containing $RuCl_3 \cdot 3H_2O$ (0.085 g, 0.325 mmol) to form a suspension. The temperature was raised to 180 °C to allow the reduction of $RuCl_3$ by the ethylene glycol. After the reduction, the suspension was diluted with 0.3 M aq. $NaNO_3$. The black solid was collected by filtration and washed with water several times.

2.3. Characterization of metallic particles and surfaces

X-ray powder diffraction (XRD) studies were performed using a Philips X'Pert diffractometer, PW3040 ($\lambda_{Cu\ K\alpha}$ = 0.15418 nm), on finely ground samples using a continuous 2θ scan mode from 35° to 90° in steps of 0.02°. XPS data were collected with a VG ESCALAB 220i-XL XPS system; samples were sputtered to ~10 nm before measurement in order to remove the effect of exposure to air. Binding energies were referenced to the Si 2p (103.4 eV) or Ti 2p (464 eV) signals [21,22]. BET analyses were performed using nitrogen adsorption and desorption, on a Micromeritics ASAP 2000 Surface and Porosity analyzer.

The temperature programmed reduction (TPR) studies were carried out in a tubular quartz microreactor connected to a mass spectrometer. In a typical TPR study, a sample (15 mg) of the catalyst was placed under a flow of 5% H_2 in Ar (20 ml/min). The temperature of the catalysts was ramped at a rate of 9 °C/min from 50 to 860 °C. The products formed during the reduction were detected by mass spectrometry.

Transmission electron microscopic (TEM) analysis was performed on a JEOL 3010 microscope at an operating voltage of 300 keV. The average particle size was determined by measuring 100 particles for each sample. TEM samples were prepared by casting a drop of the sample in ethanol onto copper grids (300 mesh) and dried at room temperature.

2.4. Catalytic studies

In a typical catalytic run, approximately 25 mg of the supported catalyst was loaded into a quartz tube reactor. The catalyst was activated by heating at 200 °C under a flow (flow rate = 140 ml/min) of air for about 1 h, and then cooled to room temperature. The catalyst activity was tested with 1% CO in air. The CO conversion was calculated on the basis of: CO conversion% = $[(CO_2)]/\{[(CO_2) + [(CO)]\}$. A Shimadzu GC-14B gas chromatograph equipped with a Carbosieve S-II column and a thermal conductivity detector was used to analyze the amount of carbon monoxide, carbon dioxide, nitrogen and oxygen.

3. Results and discussions

3.1. Characteristics of the supported catalysts

Metallic catalysts were prepared from the pyrolysis of $RuOs_3(CO)_{13}(\mu\text{-}H)_2$, $Os_3(CO)_{10}(\mu\text{-}AuPPh_3)_2$, $Os_3(CO)_{12}$, $Ru_3(CO)_{12}$ and $[Ru(CO)_4]_n$, on either silica or titania (~7 wt.% loading of precursor). A ruthenium catalyst prepared from $RuCl_3$ was used for comparison with those derived from organometallic precursors. In order to distinguish the samples obtained, the catalysts obtained are denoted as $RuOs_3/SiO_2$, $AuOs_3/SiO_2$, Os_3/SiO_2, Ru_3/SiO_2, Ru/SiO_2 and $RuCl_3/SiO_2$, respectively, for those supported on silica. The presence of osmium–ruthenium alloy, metallic osmium, or ruthenium in the samples was confirmed by XRD (Fig. S1). For instance, the XRD pattern of $AuOs_3/SiO_2$ showed peaks at 2θ = 38°, 44°, 64° and 77°, which can be assigned to the presence of cubic gold and hexagonal osmium.

The presence of RuO_2 and osmium oxides were indicated in the XPS spectra (Table 1). Thus the XPS spectra in the Os 4f core level region for the osmium-containing catalysts (Fig. 1) indicated the presence of two osmium species; one with a $4f_{7/2}$ binding energy just above 51 eV assignable to metallic osmium [22,23], and another with binding energy of ~54 eV assignable to OsO_2 [24]. The latter is probably due to oxidation on exposure to air [5,22]. We have not been able to identify the species with a binding energy of 49.8 eV observed for Os_3/TiO_2.

Similarly, for the ruthenium-containing catalysts, two ruthenium species were identified. The species with a binding energy of ~280 eV was assignable to the Ru 3d levels for Ru(0), while that with a binding energy of ~284 eV was assigned to RuO_2. The latter is again probably the result of oxidation upon exposure to air. In contrast to the osmium case, the peaks corresponding to Ru(0) and Ru(IV) were of nearly equal intensities, and may be attributed to the fact that for osmium, further oxidation of OsO_2 to form the

Table 1
XPS data for the supported catalysts.

Sample	Binding energy (eV)						
	C 1s	Ru $3d_{5/2}$		Os $4f_{7/2}$			Au $4f_{7/2}$
Ru/TiO_2	284.8	279.8	284.4	–	–		–
Ru/SiO_2	284.8	281.0	283.9	–	–		–
Ru_3/SiO_2	284.8	280.8	284.1	–	–		–
$RuOs_3/SiO_2$	284.8	280.7	283.9		51.2	54.2	–
$RuCl_3/SiO_2$	284.8	280.4	283.7	–	–		–
Os_3/TiO_2	284.8	–	–	49.8	51.3		–
Os_3/SiO_2	284.8	–	–		51.3	53.5	–
$AuOs_3/SiO_2$	284.8	–	–		51.6	53.9	84.2

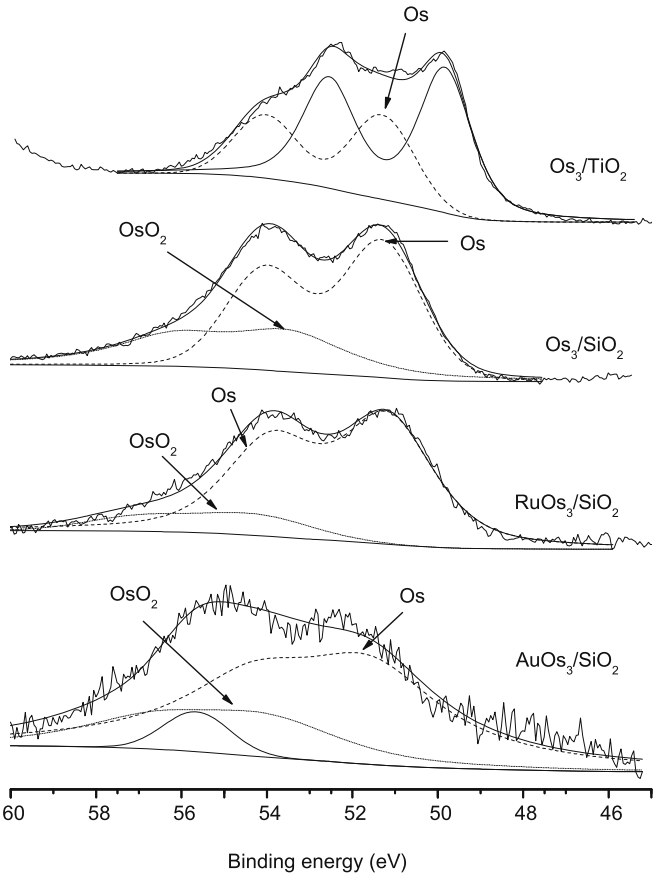

Fig. 1. XPS spectra of the osmium-containing catalysts.

volatile OsO_4 can occur more readily. For $AuOs_3/SiO_2$ the XPS spectrum also showed the Au $4f_{7/2}$ peak at a binding energy of 84.2 eV, assignable to Au(0) [25]. Finally, the XPS spectrum of $RuCl_3/SiO_2$ exhibited a Cl $2p_{3/2}$ peak at a binding energy of 195.7 eV. This is presumably a remnant from the precursory material, and is expected to affect the catalytic activity [26].

The presence of oxides was also indicated in the temperature programmed reduction curves. For instance, the hydrogen consumption profile of Ru_3/SiO_2 exhibited three peaks at 127, 252 and 410 °C, the first two of which may be assigned to unsupported and supported Ru(II)/(III) and Ru(IV) oxides, respectively [27–30]. These ruthenium oxides may have been formed on exposure to air after the preparation of catalysts [31]. Likewise, the H_2-TPR profile of Os_3/SiO_2 showed three reduction peaks at 97, 200 and 320 °C, the last being assignable to the reduction of an Os(I) species [32].

Textural parameters of the supported catalysts as determined by BET measurements, together with TEM data, are compiled in Table 2. The surface area (S_{BET}), pore volume (V_P) and average pore width (d_P(av)) are expected to decrease from the values for bare silica or titania when metallic nanoparticles are deposited onto the support. There are thus two groups of the supported catalysts that did not fit this. The first is that of Ru/TiO_2 and Ru/SiO_2, which shows slightly higher values for all three parameters, and can be attributed to the formation of nanorods from these precursors [33]. The presence of nanorods is confirmed by TEM images of both samples (Fig. S4), which show nanorods with width of ~15 nm. A second group is that of $RuCl_3/SiO_2$ and $AuOs_3/SiO_2$, particularly the former, which has larger pore volume and width than the others. We do not have a ready explanation for this, although some of the variations in the properties can be attributed to the variation in size and shapes of the metallic nanoparticles. In particular, for Os_3/TiO_2, both elongated and spherical particles were observed.

3.2. Catalytic activity

The catalytic activities of the various catalysts are presented in Fig. 2. Since the characterization above were carried out prior to catalyst activation for CO oxidation, they should properly refer to the pre-catalyst states. With the exception of $AuOs_3/SiO_2$, these catalysts showed high catalytic activity for the oxidation of CO to CO_2. The temperatures at which the CO oxidation is about 50% completed ($T_{50\%}$) are at about 60, 100, 115, 145, 190, 215, and 230 °C, for Ru/TiO_2, Ru/SiO_2, Ru_3/SiO_2, $RuOs_3/SiO_2$, Os_3/TiO_2, $RuCl_3/SiO_2$, and Os_3/SiO_2, respectively. The results suggested the following:

(i) Catalysts supported on TiO_2 were more active than those supported on SiO_2 for the same precursor. This is consistent with the observation that gold on a basic support produced a highly active catalyst [34], while that on an acidic support was inactive [35], although it was also reported that the activity over supported oxidized ruthenium was nearly independent of the support [36]. The higher activity observed on TiO_2 here may be attributed to the lower strength of CO adsorption, which would favor the CO reaction on the surface [37,38]. In the case of Os_3/SiO_2, the CO conversion dropped quickly, possibly due to the loss of osmium, which can be oxidized to the tetroxide even at room temperature; this is supported by the observed change in color of the catalyst from black to a lighter gray after use although we do not yet understand why this is not observed for osmium on titania.

(ii) Ruthenium catalysts prepared from organometallic precursors exhibited better catalytic activities than that prepared from the salt. This may be attributed to the presence of chloride in the latter; such effects have been attributed to selective blockage of active sites and chloride-induced structural rearrangements [39,40].

(iii) Ruthenium showed better catalytic activity than osmium. The addition of ruthenium to osmium decreased the CO conversion temperature.

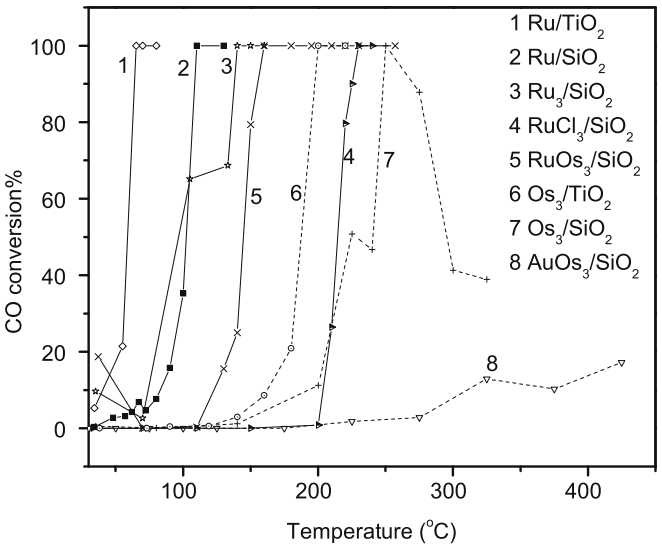

Fig. 2. CO oxidation on the supported catalysts.

Table 2
Textural properties and TEM data of supported catalysts and naked supports.

Sample	Textural properties[a]			TEM data (nm)
	S_{BET} ($m^2\ g^{-1}$)	V_P ($cm^{-3}\ g^{-1}$)	d_P(av) (Å)	
SiO_2	210	0.42	81	–
Ru/SiO_2	210	0.51	98	~15 (width)
Ru_3/SiO_2	160	0.33	85	4.0
Os_3/SiO_2	120	0.28	95	2.6
$RuOs_3/SiO_2$	140	0.33	95	3.1
$AuOs_3/SiO_2$	190	0.59	130	4.5
$RuCl_3/SiO_2$	200	1.30	260	1.6
TiO_2	48	0.11	98	–
Ru/TiO_2	52	0.16	130	~15 (width)
Os_3/TiO_2	44	0.11	98	–[b]

[a] S_{BET} = surface area; V_P = pore volume; and d_P(av) = average pore width.
[b] Shapes were irregular.

For $AuOs_3/SiO_2$, the CO conversion was about 17% at 425 °C, which appears to be at odds with observations that metallic Au NPs with size <5 nm exhibit good catalytic activity [41]. However, this may be attributed to the presence of osmium so that the particle size does not reflect that of pure gold. Furthermore, it suggested that the catalyst cannot be regarded as segregated osmium and gold phases, but rather as a bimetallic osmium–gold alloy phase which behaved like neither metal.

4. Conclusions

Supported catalysts containing osmium and/or ruthenium showed good catalytic activity for CO oxidation. The catalytic activity followed the order Ru > $RuOs_3$ > Os ≫ $AuOs_3/SiO_2$. In particular, ruthenium catalysts prepared from organometallic precursors exhibited better activity than that prepared from $RuCl_3$. Furthermore, ruthenium supported on TiO_2 exhibited the best catalytic activity at the lowest operating temperature. The good control of particle size, and the absence of residual ions that may act as

poison, demonstrate that organometallic clusters can serve as excellent precursors for the preparation of very active metallic catalysts.

Acknowledgments

This work was supported by an A*STAR grant (Research Grant No. 022 109 0061) and one of us (C.L.) thanks the University for a Research Scholarship.

Appendix A. Supplementary material

Supplementary data associated with this article can be found, in the online version, at doi:10.1016/j.jorganchem.2009.03.038.

References

[1] W. Shen, J. Shi, H. Chen, J. Gu, Y. Zhu, X. Dong, Chem. Lett. 34 (2005) 390.
[2] NIST-JANAF Thermochemical Tables, fourth ed., Part 1 Al-Co, p. 641.
[3] M. Haruta, Catal. Today 36 (1997) 153.
[4] T.V.W. Janssens, B.S. Clausen, B. Hvolbæk, H. Falsig, C.H. Christensen, T. Bligaard, J.K. Nørskov, Top. Catal. 44 (2007) 15.
[5] S.Y. Chin, O.S. Alexeev, M.D. Amiridis, Appl. Catal. A 286 (2005) 157.
[6] R.S. Sundar, S. Deevi, J. Nanopart. Res. 8 (2006) 497.
[7] A.N. Ilichev, A.A. Firsova, V.N. Korchak, Kinet. Catal. 47 (2006) 585.
[8] T. Schalow, B. Brandt, M. Laurin, S. Schauermann, J. Libuda, H. Freund, J. Catal. 242 (2006) 58.
[9] E. Ko, E.D. Park, K.W. Seo, H.C. Lee, D. Lee, S. Kim, Catal. Today 116 (2006) 377.
[10] E. Ko, E.D. Park, K.W. Seo, H.C. Lee, D. Lee, S. Kim, Catal. Lett. 110 (2006) 275.
[11] J.W. Saalfrank, W.F. Maier, C.R. Chimie 7 (2004) 483.
[12] L. Zhang, H. Kisch, Angew. Chem., Int. Ed. Engl. 39 (2000) 3921.
[13] D.J. Suh, T. Park, W. Kim, I. Hong, J. Power Sources 117 (2003) 1.
[14] A.C.W. Koh, W.K. Leong, L. Chen, T.P. Ang, J. Lin, B.F.G. Johnson, T. Khimyak, Catal. Commun. 9 (2008) 170.
[15] A. Siani, B. Captain, O.S. Alexeev, E. Stafyla, A.B. Hungria, P.A. Midgley, J.M. Thomas, R.D. Adams, M.D. Amiridis, Langmuir 22 (2006) 5160.
[16] J.M. Ramallo-Lopez, G.F. Santori, L. Giovanetti, M.L. Casella, O.A. Ferretti, F.G. Requejo, J. Phys. Chem. B 107 (2003) 11441.
[17] L. Pereira, W.K. Leong, S.Y. Wong, J. Organomet. Chem. 609 (2000) 104.
[18] K. Burgess, R.P. White, Inorg. Synth. 27 (1990) 209.
[19] N. Masciocchi, M. Moret, P. Cariati, F. Ragaini, A. Sironi, J. Chem. Soc., Dalton Trans. (1993) 471.
[20] W.R. Hastings, M.C. Baird, Inorg. Chem. 25 (1986) 2913.
[21] P. Reys, H. Rojas, React. Kinet. Catal. Lett. 88 (2006) 363.
[22] J. Huang, H. Yang, Q. Huang, Y. Tang, T. Lu, D.L. Akins, J. Electrochem. Soc. 151 (2004) A1810.
[23] Y. Zhu, C.R. Cabrera, Electrochem. Solid-State Lett. 4 (2001) A45.
[24] A. Hamnett, B.J. Kennedy, Electrochim. Acta 33 (1988) 1613.
[25] C.D. Wagner, W.M. Riggs, L.E. Davis, J.M. Moulder, G.E. Muilenberg (Eds.), Handbook of X-Ray Photoelectron Spectroscopy, Perkin–Elmer Co., Eden, Prairie, 1979.
[26] P. Broqvist, L.M. Molina, H. Gronbeck, B. Hammer, J. Catal. 227 (2004) 217.
[27] X. Fu, H. Yu, F. Peng, H. Wang, Y. Qian, Appl. Catal. A 321 (2007) 190.
[28] V. Mazzieri, F. Coloma-Pascual, A. Arcoya, P.C. L'Argentiere, N.S. Figoli, Appl. Surf. Sci. 210 (2003) 222.
[29] P. Betancourt, A. Rives, R. Hubaut, C.E. Scott, J. Goldwasser, Appl. Catal. A 170 (1998) 307.
[30] J.M. Rynkowski, T. Paryjczak, M. Lenik, Appl. Catal. A 126 (1995) 257.
[31] P.G.J. Koopman, A.P.G. Kieboom, H. van Bekkum, J. Catal. 69 (1981) 172.
[32] D. Eliche-Quesada, J.M. Merida-Robles, E. Rodriguez-Castellon, A. Jimenez-Lopez, Appl. Catal. A 279 (2005) 209.
[33] C. Li, W.K. Leong, Langmuir 24 (2008) 12040.
[34] D. Andreeva, V. Idakiev, T. Tabakova, L. Ilieva, P. Falaras, A. Bourlinos, A. Travlos, Catal. Today 72 (2002) 51.
[35] A. Wolf, F. Schuth, Appl. Catal. A 226 (2002) 1.
[36] J. Assmann, E. Loffler, A. Birkner, M. Muhler, Catal. Today 85 (2003) 235.
[37] S.H. Oh, G.B. Fisher, J.E. Carpenter, D.W. Goodman, J. Catal. 100 (1986) 360.
[38] S.H. Oh, R.M. Sinkevitch, J. Catal. 142 (1993) 254.
[39] E.T. Iyagba, T.E. Hoost, J.U. Nwalor, J.G. Goodwin Jr., J. Catal. 123 (1990) 1.
[40] J.A. Mieth, J.A. Schwarz, J. Catal. 118 (1989) 218.
[41] M. Haruta, S. Tsubota, T. Kobayashi, H. Kageyama, M.J. Genet, B. Delmon, J. Catal. 144 (1993) 175.